Check for updates

Received: 7 December 2023 | Revised: 26 January 2024 | Accepted: 31 January 2024

DOI: 10.1002/bit.28673

ARTICLE

BIOTECHNOLOGY and BIOENGINEERING WILEY

A low-temperature SPR-based assay for monoclonal antibody galactosylation and fucosylation assessment using FcγRIIA/B

Jimmy Gaudreault[1] | Catherine Forest-Nault[1] | Michel Gilbert[2] | Yves Durocher[3] | Olivier Henry[1] | Gregory De Crescenzo[1]

[1]Department of Chemical Engineering, Polytechnique Montréal, Montréal, Quebec, Canada

[2]Human Health Therapeutics Research Center, National Research Council Canada, Ottawa, Ontario, Canada

[3]Human Health Therapeutics Research Center, National Research Council Canada, Montréal, Québec, Canada

Correspondence
Olivier Henry
Email: olivier.henry@polymtl.ca

Gregory De Crescenzo
Email: gregory.decrescenzo@polymtl.ca

Funding information
Natural Sciences and Engineering Research Council of Canada

Abstract

Monoclonal antibodies (MAbs) are powerful therapeutic tools in modern medicine and represent a rapidly expanding multibillion USD market. While bioprocesses are generally well understood and optimized for MAbs, online quality control remains challenging. Notably, N-glycosylation is a critical quality attribute of MAbs as it affects binding to Fcγ receptors (FcγRs), impacting the efficacy and safety of MAbs. Traditional N-glycosylation characterization methods are ill-suited for online monitoring of a bioreactor; in contrast, surface plasmon resonance (SPR) represents a promising avenue, as SPR biosensors can record MAb–FcγR interactions in real-time and without labeling. In this study, we produced five lots of differentially glycosylated *Trastuzumab* (TZM) and finely characterized their glycosylation profile by HILIC-UPLC chromatography. We then compared the interaction kinetics of these MAb lots with four FcγRs including FcγRIIA and FcγRIIB at 5°C and 25°C. When interacting with FcγRIIA/B at low temperature, the differentially glycosylated MAb lots exhibited distinct kinetic behaviors, contrary to room-temperature experiments. Galactosylated TZM (1) and core fucosylated TZM (2) could be discriminated and even quantified using an analytical technique based on the area under the curve of the signal recorded during the dissociation phase of a SPR sensorgram describing the interaction with FcγRIIA (1) or FcγRII2B (2). Because of the rapidity of the proposed method (<5 min per measurement) and the small sample concentration it requires (as low as 30 nM, exact concentration not required), it could be a valuable process analytical technology for MAb glycosylation monitoring.

KEYWORDS

fucosylation, galactosylation, glycosylation monitoring, kinetics analysis, monoclonal antibodies (MAbs), surface plasmon resonance (SPR)

Olivier Henry and Gregory De Crescenzo contributed equally to this study.

This is an open access article under the terms of the Creative Commons Attribution-NonCommercial-NoDerivs License, which permits use and distribution in any medium, provided the original work is properly cited, the use is non-commercial and no modifications or adaptations are made.
© 2024 The Authors. *Biotechnology and Bioengineering* published by Wiley Periodicals LLC.

1 | INTRODUCTION

According to the Umabs Antibody Therapies Database (Umabs—DB, https://umabs.com/), 340 therapies based on monoclonal antibodies (MAbs) have been approved by at least one regulatory agency as of September 2023 (Umabs, 2023). Of these, 157 use whole antibodies, while the rest use fragments or fusion proteins. These drugs are mainly indicated for the treatment of chronic diseases and cancer (Lyu et al., 2022), but other fields have been explored (Mullard, 2021). The global market size of Mabs has increased by 500-fold in the last 20 years, reaching 186 billion USD in 2021 (Lyu et al., 2022), and is expected to reach 300 billion USD by 2025 (Carrara et al., 2021) as more new MAbs enter clinical trials (more than 100 MAbs entered clinical trials for each year between 2015 and 2020 (Mullard, 2021)). Moreover, a large amount of patents pertaining to MAbs have expired or will expire in the near future, opening the market to biosimilars (Gherghescu & Delgado-Charro, 2021; Moorkens et al., 2020), 103 of them having already been approved by at least one regulatory agency (Umabs, 2023). On top of therapeutic applications, MAbs are also used for diagnostic and theranostic applications (Farahavar et al., 2019), making them one of the most versatile and powerful tools in modern medicine.

Most therapeutic MAbs are of the immunoglobulin G subclass (IgG) (Boune et al., 2020). Their Fc domain recruits other parts of the immune system via interactions with membrane-bound Fc receptors. Of those, Fcγ receptors (FcγRs) play an important role in the efficacy and safety of an MAb-based therapeutic. Notably, FcγRIII (CD16) is present at the surface of natural killer cells and mediates antibody-dependent cytotoxicity (ADCC), while FcγRIIA and FcγRIIB (CD32A/B) mediate the activation and the inhibition of the phagocytosis activity, respectively. The dynamics and affinity of the IgG–FcγR interaction are strongly affected by the N-glycosylation state of the IgG, making glycosylation a critical quality attribute of MAbs (Forest-Nault et al., 2021).

Glycosylation is a posttranslational modification regulated by the cellular glycosylation machinery (Varki, 2017). In the case of antibodies, glycan chains are added to the heavy chain in the CH2 domain of the highly conserved Fc region on the asparagine residue at position 297. The exact nature of the glycans added is highly heterogeneous and dependent on the host-cell type and the cell culture conditions in the bioreactor (temperature, pH, cell media components, feed strategy, etc.) (Hossler et al., 2009). Therefore, a mixture of different glycoforms of the same MAb is obtained at the end of the production process. Glycosylation influences immunogenicity and clearance (Ghaderi et al., 2010; Goetze et al., 2011), and effector functions such as ADCC and complement-dependent cytotoxicity (CDC) (Hodoniczky et al., 2005; Shade & Anthony, 2013; Yamane-Ohnuki et al., 2004). Notably, removal of core fucose strengthens MAb interactions with FcγRIIIA, therefore, improving ADCC, and galactosylation promotes CDC activity.

It follows that measuring MAb glycosylation during production is of great interest to ensure safety and efficacy of the product, as well as batch-to-batch repeatability and biosimilar equivalency. This is in line with the principles of quality by design (U. S. Food and Drug Administration, 2009) and process analytical technologies (PAT) (U. S. Food and Drug Administration, 2004) introduced by the Food and Drug Administration. However, typical techniques based on chromatography and mass spectrometry are ill-suited for real-time glycosylation monitoring in a bioreactor because of their need for labeling and their laborious and lengthy workflow (Kaur, 2021). Be that as it may, frameworks allowing chromatography-based glycosylation analysis online of a bioreactor and the required sample processing steps have been suggested (Gyorgypal & Chundawat, 2022; Tharmalingam et al., 2015).

Nevertheless, we believe that surface plasmon resonance (SPR) biosensing remains an interesting avenue. Indeed, its ability to measure protein–protein interactions in real-time and without labels with small sample volumes are hallmarks of a promising PAT tool that could be used all throughout the development and production processes of MAbs (Gaudreault, Forest-Nault, et al., 2021). In an SPR assay, an analyte injection phase (association phase) is followed by an injection of buffer that allows measurement of the dissociation kinetics (dissociation phase). The resulting sensorgram can be used to calculate the thermodynamic and kinetic constants describing the analyte–ligand interaction. Of interest, our group has previously demonstrated the potential of SPR detection for bioprocess monitoring by harnessing an SPR biosensor to a bioreactor (Chavane et al., 2008; Jacquemart et al., 2008). The SPR technique has also been coupled with size exclusion chromatography (SEC) (Lakayan et al., 2016), a combination of liquid chromatography and mass spectroscopy (Lakayan et al., 2018), and asymmetric flow field-flow fractionation (Leeman et al., 2021), demonstrating its adaptability.

The IgG–FcγR interaction has been the subject of many SPR studies (Forest-Nault et al., 2021), most of these involving immobilizing an FcγR and injecting different antibody glycoforms to compare their binding kinetics and/or affinity for various receptors (Cambay et al., 2019, 2020; Falconer et al., 2018; Kanda et al., 2007; Okazaki et al., 2004; Shibata-Koyama et al., 2009; Subedi & Barb, 2016). To evaluate the effect of glycosylation on IgG–FcγR interactions, one may use chemoenzymatic glycoengineering techniques to produce IgG lots with varying glycosylation profiles. However, the ability to infer an otherwise unknown glycosylation profile from SPR data remains to be demonstrated. The latter is what would be necessary to implement a glycosylation monitoring tool based on SPR biosensing.

Interestingly, it has been widely reported that SPR data of the IgG–FcγR interaction do not follow a 1:1 interaction scheme (Forest-Nault et al., 2021), obfuscating the meaning of kinetic parameters derived in such a way. This is not surprising considering the high degree of heterogeneity in MAb glycosylation and its impact upon MAb interaction with the FcγRs.

In this manuscript, we hypothesize that data analysis techniques based on the shape of the SPR signal (i.e., model-free) are preferable over comparing parameters identified with ill-fitting models. Specifically, we turned our attention to the area under the curve (AUC) of the dissociation phase of the signal. The dissociation phase signal is particularly interesting as we have demonstrated that its shape (not to be confused with its amplitude) is independent of analyte concentration. We further combined this approach with kinetic investigations at low temperature (5°C), as our group previously showed that slowing kinetics facilitates discrimination between SPR signals of different analytes for a given ligand (Gaudreault

10970290, 0, Downloaded from https://analyticalsciencejournals.onlinelibrary.wiley.com/doi/10.1002/bit.28673 by Ecole Polytech De Montreal, Wiley Online Library on [18/03/2024]. See the Terms and Conditions (https://onlinelibrary.wiley.com/terms-and-conditions) on Wiley Online Library for rules of use; OA articles are governed by the applicable Creative Commons License

et al., 2022). In this work, we found that the AUC during dissociation was proportional to the IgG galactosylation level when using a FcγRIIA surface and that the AUC during dissociation correlated with the IgG core fucosylation level when using a FcγRIIB surface. Variations in AUC due to differential glycosylation were amplified at 5°C. Interestingly, the AUC conclusions matched well-known results pertaining to binding affinity (i.e., core fucose diminished both the AUC and the binding affinity with FcγRIIIA). Of special interest, the AUC approach requires only one IgG concentration (which may be unknown) whereas affinity identification requires multiple experiments at known concentrations.

The proposed methodology was tested using differentially glycosylated and finely characterized lots of *Trastuzumab* (TZM), a monoclonal IgG1. The experiments were performed using our in-house SPR assay based on the capture of Ecoil-tagged FcγRs via coiled-coil interactions (Murschel et al., 2013). This study demonstrates two novel notions in the field of SPR data analysis: (1) conducting the experiments at a lower temperature to slow the kinetics accentuates differences in the signals and (2) analyzing the shape of the signal rather than fitting a model, to compare the kinetic behavior of two analytes. Hence, we believe it could stimulate research both in the fields of MAb N-glycosylation profiling and SPR data analysis.

2 | METHODOLOGY

2.1 | Chemical reagents and biological material

Sodium acetate (#S2889), sodium tetraborate (#229946), guanidium hydrochloride (#G3272), ethanolamine hydrochloride (#E6133), and DL-cysteine (#861677) were purchased from Sigma-Aldrich. N-hydroxysuccinimide (NHS, #24500) and 1-ethyl-3-(3-dimethylaminopropyl) carbodiimide hydrochloride (EDC, #22980) were purchased from Thermo Fisher Scientific. 2-(2-pyridinyldithio) ethaneamine hydrochloride (PDEA, #BR100058) and HBS-EP buffer (0.01 M HEPES pH 7.4, 0.15 M NaCl, 3mM EDTA, 0.005% v/v surfactant P20, #BR100669) were acquired from Cytiva. Acetate, borate, and HBS-EP buffers were prepared with ultrapure MiliQ water (Millipore Gradient A10 purification system) and filtered with 0.22 µm polyethersulfone membranes.

Kcoil peptide with a terminal cysteine (CGG-$(KVSALKE)_5$) was synthesized at the University of Sherbrooke (QC, Canada) with a Symphony X solid-phase peptide synthesizer (Gyros Protein Technologies). Kcoil was purified by preparative inverse-phase high-performance liquid chromatography and characterized by mass spectroscopy. The final purity is >99.9%.

2.2 | Protein expression and purification

2.2.1 | Plasmids

cDNA coding for TZM light chain and TZM heavy chain were cloned into individual pTT5® vectors, as well as the cDNA corresponding to the human glycosyltransferase β1,4-galactosyltransferase 1 (GT) (Cambay et al., 2019; Zhang et al., 2009).

FcγRIIA, FcγRIIB, FcγRIIIA (either bearing a valine (V158) or a phenylalanine (F158) at position 158) constructs contained the $(EVSALEK)_5$ peptide sequence necessary for the coiled-coil ligand capture strategy, and a 10-histidine C-terminal tag. The codon-optimized sequences encoding these constructs were also cloned into pTT5 vectors (Cambay et al., 2019).

2.2.2 | Cell culture

FcγRs and TZM glycoforms were transiently produced in CHO^{55E1} cells and glycoengineered CHO cell lines following a previously reported protocol (Stuible et al., 2021). In brief, cells were seeded at 1×10^6 cells/mL 2 days before transfection in a chemically defined proprietary media formulation supplemented with 4 mM L-glutamine and incubated in shake flasks (Corning, NY, USA) under agitation (120 rpm) at 37°C, 5% CO_2. On the day of transfection, when the cell density achieved was ~8×10^6 cells/mL, cells were diluted with 25% fresh media and dimethylacetamide was added to 0.083% (v/v). Cell cultures returned to the incubator while the DNA mix was prepared. PEI-Max (Polysciences) was used to transfect cells at a DNA:PEI (polyethylenimine) ratio of 1:7 (w:w) and the final concentration of plasmid DNA in the cell culture media was 1.4 µg/mL. The transfected DNA was a mix of 85% (w/w) pTT5-HC and pTT5-LC (ratio HC:LC of 1:1) or FcγR-E5 constructs, 10% pTT-Bcl-XL (antiapoptotic effector) and 5% pTT-GFP. At 24 h posttransfection, all cultures were supplemented with anticlumping supplement (1:500 dilution) (Irvine Scientific) as well as Feed 4 (2.5% v/v) (Irvine Scientific) before moving to a 32°C incubator. At 5 days post-transfection, cultures were fed with additional 5% of Feed 4 and additional glucose was added every 2–3 days to maintain a minimal concentration of 17 mM. Cell supernatants were collected at 6–7 days posttransfection.

The human GT expression vector was co-transfected with TZM vectors for transient expression of galactosylated TZM (TZM-GT). The glycoengineered Fut8 knock-out cell line, the Fut8 and ST3Gal4 double knock-out cell line (dKO2) and the dKO2/ST6 cell line, which stably expresses the human ST6Gal1 gene, were derived from CHO^{55E1} using CRISPR/Cas9 as described elsewhere (Koyuturk et al., 2022). These cell lines were used for transient expression of different afucosylated TZM lots (Afuc1, Afuc2, Afuc3).

2.2.3 | Protein purification

E5-tagged FcγRs were harvested and centrifuged at 3300*g* for 20 min. Supernatants were filtered through 0.45 µm membranes. The clarified supernatants were purified by IMAC with 1 mL Nickel Sepharose Excel resin (GE Healthcare) as described elsewhere (Cambay et al., 2020). Columns were equilibrated with equilibration buffer (50 mM NaPO4 pH 7.8, 300 mM NaCl) and supernatants were

10970290, 0, Downloaded from https://analyticalsciencejournals.onlinelibrary.wiley.com/doi/10.1002/bit.28673 by Ecole Polytech De Montreal, Wiley Online Library on [18/03/2024]. See the Terms and Conditions (https://onlinelibrary.wiley.com/terms-and-conditions) on Wiley Online Library for rules of use; OA articles are governed by the applicable Creative Commons License

loaded at 3 mL/min. Columns were washed once with 50 mM NaPO4 pH 7.8, containing 300 mM NaCl and 10 mM imidazole and eluted with the same buffer containing 300 mM imidazole. Fractions containing the receptors were pooled and the elution buffer was changed to PBS with a desalting NAP-25 column (GE Healthcare). Purified FcγRs were concentrated with Amicon Ultra-4 10 K centrifugal filter units (Millipore) and further purified by SEC using a Superdex75 10/300 G L column (GE Healthcare) to remove aggregates. The column was equilibrated with PBS and 0.5 mL of sample was loaded onto the column at 1 mL/min. PBS was used to elute the proteins.

All TZM lots were harvested and purified following a previously described protocol (Cambay et al., 2019). A total of 2 mL MabSelect SuRe columns (GE Healthcare) were equilibrated with PBS. IgGs were harvested, centrifuged at 3300*g* and filtered through 0.45 µm membranes before they were loaded onto the equilibrated columns. The columns were then washed with PBS and antibodies were eluted with 100 mM citrate buffer at pH 3. The fractions containing the IgGs were pooled and the citrate buffer was changed to PBS with a desalting NAP-25 column (GE Healthcare). Purified MAbs were concentrated with Amicon Ultra-4 30 K centrifugal filter units (Millipore) and aggregates were separated by SEC using a Superdex200 column (GE Healthcare). The column was equilibrated with PBS and 5 mL of sample was loaded at 1.5 mL/min. PBS buffer was used to elute the proteins.

All purified samples were quantified by absorbance at 280 nm using a Nanodrop spectrophotometer (Thermo Fisher Scientific), sterile-filtered, aliquoted and stored at −80°C.

2.2.4 | Glycan analyses by HILIC-UPLC

Glycans were released from the glycoproteins, as previously described (Koyuturk et al., 2022), using Rapid PNGase F (New England BioLabs, cat# P0710) at 50°C for 10 min, after a 2 min denaturation step at 80°C. The PNGase F and proteins were removed with a 50 or 250 mg Discovery glycan SPE column (Millipore-Sigma), and the glycans were dried under vacuum. They were then labeled with 2-aminobenzamide (2-AB) (Sigma-Aldrich, cat# PP0520) and further purified (Bigge et al., 1995). The 2-AB labeled samples (excluding the human IgG control) were treated with α2-3,6,8 neuraminidase (MNV-02) and α1-2,3,6 mannosidase (New England Biolabs, cat# P0768S) to identify peaks containing sialic acid and high-mannose glycoforms. Glycans were analyzed by HILIC with fluorescent detection using an Acquity UPLC wide-pore glycoprotein BEH amide (Waters Corp., cat# 176003702) and a Vanguard glycoprotein BEH amide guard column (Waters, cat# 176003699) with the column heated to 60°C and a flow rate of 0.5 mL/min. Glycans were eluted using 50 mM ammonium formate, pH 4.4 (mobile phase A) and 100% acetonitrile (mobile phase B) starting with an initial ratio of 78%–55.9% B over 43.5 min. Peaks were calibrated with a 2-AB labeled dextran ladder standard (Waters Corp., cat# 186006841) and compared to GU values in a database (https://www.glycostore.org/collections) of previously ran samples of known composition.

2.3 | SPR experiments

All SPR experiments conducted in this study were performed using a Biacore T100 biosensor with a CM5 sensor chip bearing carboxymethylated dextran (Cytiva). This biosensor makes use of the geometry proposed by Kretschmann and Raether (De Crescenzo et al., 2008; Homola, 2003). The running buffer for all experiments was HBS-EP, and the data acquisition rate was set to 10 Hz. The experimental temperature was set to either 5°C or 25°C, as indicated. A de novo coiled-coil scheme was used to capture the Ecoil-tagged FcγRs by first covalently grafting Kcoil peptides on the biosensor surface.

2.3.1 | Kcoil grafting

Kcoil was covalently grafted by thiol coupling chemistry according to a previously published protocol (Dégardin et al., 2023; Murschel et al., 2013). The procedure was performed on two of the four channels available on the CM5 chip. Briefly, the carboxyl groups of the chip were first activated by injecting a 1:1 (v/v) mixture of 0.4 M EDC and 0.1 M NHS for 7 min at a flow rate of 5 µL/min. Then, a solution containing 1.8 mg of the thiol coupling reagent PDEA dissolved in 150 µL of 50 mM borate pH 8.5 was injected for 8 min at 5 µL/min. Next, ethanolamine (1 M, pH 8.5) was injected (4 min, 5 µL/min) to deactivate the remaining carboxyl sites. Kcoil was diluted in acetate buffer (100 mM, pH 4.5) at a concentration of 167 µg/mL and injected in short pulses of 20 µL/min until an immobilization density of approximately 1800 Resonance Units was reached (RU, where 1 RU is equivalent to approximately 1 pg/mm^2 of immobilized protein). The remaining PDEA molecules were blocked by an injection of a solution obtained by diluting 3 mg of DL-cysteine and 14 mg of NaCl in 500 µL of acetate buffer (100 mM, pH 4.5). Finally, multiple 15 s pulses of 6 M guanidium-HCl were performed at 100 µL/min to clear all unreacted species that remained near the surface. A final Kcoil immobilization density of approximately 1500 RU was reached with this process. Ample amounts of running buffer were injected before and after to ensure the biosensor was well equilibrated.

2.3.2 | FcγRs capture rate

The capture rate of all E-coil tagged FcγRs (FcγRIIA, FcγRIIB, V158, F158) on the Kcoil surface was tested at both 5°C and 25°C by injecting the receptor for 25 s at 5 µL/min and observing the capture level reached. Assuming a constant capture rate, the injection time required to reach 20 RU of FcγRs was determined. This level was selected as it was sufficient to record SPR sensorgrams with an acceptable signal-to-noise ratio, while low enough to avoid mass transport limitations.

10970290, 0, Downloaded from https://analyticalsciencejournals.onlinelibrary.wiley.com/doi/10.1002/bit.28673 by Ecole Polytech De Montreal, Wiley Online Library on [18/03/2024]. See the Terms and Conditions (https://onlinelibrary.wiley.com/terms-and-conditions) on Wiley Online Library for rules of use; OA articles are governed by the applicable Creative Commons License

2.3.3 | SPR assay to study the IgG–FcγR interaction

Each SPR cycle started with the capture of the FcγR (ligand) on only one of the two Kcoil SPR surfaces. The second surface was kept ligand-free for referencing purposes. TZM glycoforms (analytes) were then injected at 30 μL/min for 30 s (FcγRIIA and FcγRIIB), 300 s (V158) or 180 s (F158). This analyte injection phase is commonly called the association phase. Next, the running buffer was injected at 30 μL/min for 60 s (FcγRIIA and FcγRIIB), 500 s (V158) or 240 s (F158). This corresponds to the dissociation phase. The phase durations were selected for each FcγR based on its typical binding kinetics. Finally, the surface was regenerated via two 15 s injection of 6 M guanidium-HCl. This returned the SPR signal to its basal level (i.e., the FcγRs and antibodies were removed, but not the Kcoil). This cycle was repeated for every SPR sensorgram recorded in this study. Cycles with a blank analyte injection (running buffer) were performed to allow double referencing (Myszka, 1999).

2.4 | SPR data analysis

2.4.1 | Equilibrium constant

For each TZM glycoform, a series of five concentrations (C_{TOT}) (10, 30, 100, 300, and 1000 nM) were injected over all receptors until an equilibrium plateau was reached. The plateau values $R_{EQ,TOT}$ (in RU) were recorded, and the steady-state model was used to determine the affinity of the IgG–FcγR interaction ($K_{A,\text{obs}}$):

$$R_{EQ,TOT} = \frac{K_{A,\text{obs}} R_{\max,\text{obs}} C_{TOT}}{1 + K_{A,\text{obs}} C_{TOT}}.$$

Here, $R_{\max,\text{obs}}$ is the theoretical SPR signal (in RU) that would be reached if all immobilized ligand molecules interacted with an analyte molecule. $K_{A,\text{obs}}$ and $R_{\max,\text{obs}}$ were identified using an in-house Matlab program via optimization, given a series of known $R_{EQ,TOT}$ and C_{TOT} values.

2.4.2 | AUC

To calculate the AUC of the dissociation phase of an SPR sensorgram, a numerical integration of the signal was computed using the trapezoidal method ("cumtrapz" function in Matlab). To avoid bias from bulk shift artifacts caused by the changing of injected solutions at the end of the association phase, the first 0.5 s of the dissociation phase were excluded.

2.4.3 | Normalization of SPR sensorgrams

The SPR sensorgrams were normalized in two ways before AUC computation. First, for data obtained with FcγRIIA/B, the sensorgrams were translated to 0 at the end of the sensorgram by subtracting the average of the last 25 s of the signal from the whole sensorgram. This removed bias resulting in convergence to a nonzero response at the end of the sensorgram, possibly due to ligand leaving the surface, a slight temperature drift, or a minute variation in the running buffer. Second, the sensorgrams were normalized to 100% at the end of the association phase by taking the average over 3–1 s before the end of the association phase. This procedure canceled effects caused by small cycle-to-cycle variations in the FcγR capture level. Crucially, it allowed comparison of AUCs computed with different IgG concentrations, as we demonstrate in this study that the dissociation signal (when normalized) is not dependant on the IgG concentration when equilibrium is reached at the end of the association phase.

2.4.4 | Mathematical rationalization of the AUC as an inference metric

IgG–FcγR interaction sensorgrams do not properly fit a simple 1:1 Langmuir model (Forest-Nault et al., 2021), hence the need for more complex models and data analysis schemes. Most complex models amount to a sum of decaying exponentials during the dissociation phase of the signal. For example, assuming an IgG solution contains a heterogeneous mixture of antibody glycoforms, each will compete to bind the FcγR, exhibiting unique affinities. The contribution to the SPR signal at equilibrium of glycoform i ($R_{EQ,i}$) is:

$$R_{EQ,i} = \frac{F_i K_{A,i} R_{\max,i} C_{TOT}}{1 + K_{A,\text{obs}} C_{TOT}}.$$

The observed affinity ($K_{A,\text{obs}}$) corresponds to the average of affinities ($K_{A,i}$) weighted by their proportion in the mixture (F_i):

$$K_{A,\text{obs}} = \sum_{i=1}^{N} F_i K_{A,i}.$$

Further, $R_{\max,i} \approx R_{\max,\text{obs}}$ because, for proteins, the maximal SPR signal is proportional to the molecular weight. Different glycoforms of a given IgG have very similar weights, as the glycans represent only a small proportion of the total molecular weight. Hence the theoretical maximal SPR response ($R_{\max,i}$) can be considered the same for all glycoforms. The proportion of the observed SPR response at equilibrium due to a single glycoform i (Z_i) is thus:

$$Z_i = \frac{R_{EQ,i}}{R_{EQ,TOT}} = \frac{F_i K_{A,i} R_{\max,i}}{K_{A,\text{obs}} R_{\max,\text{obs}}} = \frac{F_i K_{A,i}}{K_{A,\text{obs}}}.$$

Normalized to 1, the analytical expression of the dissociation signal is:

$$R_{\text{Norm}}(t) = \sum_{i=1}^{N} Z_i e^{-k_{d,i} t},$$

where $k_{d,i}$ is the dissociation rate of glycoform i. To compute the AUC, we take the integral between the beginning ($t = 0$) and the end ($t = t_{\text{end}}$) of the dissociation phase:

10970290, 0, Downloaded from https://analyticalsciencejournals.onlinelibrary.wiley.com/doi/10.1002/bit.28673 by Ecole Polytech De Montreal, Wiley Online Library on [18/03/2024]. See the Terms and Conditions (https://onlinelibrary.wiley.com/terms-and-conditions) on Wiley Online Library for rules of use; OA articles are governed by the applicable Creative Commons License

$$\int_0^{t_{end}} R_{\mathrm{Norm}}(t)\mathrm{d}t = \sum_{i=1}^{N} \frac{Z_i}{k_{d,i}} e^{-0} + \sum_{i=1}^{N} -\frac{Z_i}{k_{d,i}} e^{-k_{d,i} t_{end}}.$$

Assuming the signal goes to 0 RU at the end of the dissociation, the second right-hand term is equal to 0. The result of the integral is independent from C_{TOT}. Rather, it is directly correlated to the composition of the mixture and to the glycoform-specific parameters of the IgG–FcγR interaction:

$$\int_0^{t_{\mathrm{end}}} R_{\mathrm{Norm}}(t)\mathrm{d}t = \sum_{i=1}^{N} \frac{Z_i}{k_{d,i}} = \sum_{i=1}^{N} \frac{F_i K_{A,i}}{k_{d,i} K_{A,\mathrm{obs}}}.$$

To prove this result experimentally, the AUC was computed for all glycoforms at different antibody concentrations, and the findings (i.e., which glycoform has more AUC for a given FcγR) and the AUC values were found to be robust (see Section 3).

3 | RESULTS

3.1 | N-linked glycans analysis with HILIC-UPLC

We produced five lots of TZM, each with different glycosylation profiles obtained through glycoengineering techniques, as described in the Methods section. We then finely characterized their glycosylation profile via HILIC-UPLC (see Methods). The results are reported in Figure 1. The wild-type TZM (TZM-WT) is highly fucosylated (more than 90% of antibodies contain a core fucose). TZM-GT is also highly fucosylated (75%) but contains a larger proportion of terminal galactose (68.3%). TZM-GT also contains a considerable proportion of high mannose glycoforms (20.9%). The remaining three glycoforms (TZM-Afuc1, TZM-Afuc2, TZM-Afuc3) were produced by glycoengineered cell lines that cannot perform core fucosylation. The HILIC-UPLC results are summarized in Table 1 and shown in detail in Supporting Information S1: Figure S1.

3.2 | Lowering SPR experimental temperature facilitates signal differentiation

Having characterized the TZM glycoforms, we then performed the SPR experiments by immobilizing a low density (around 20 RU) of FcγRs to avoid mass transport limitations.

In a previous work (Gaudreault et al., 2022), we demonstrated that lower experimental temperatures amplify the differences in kinetic behavior between a ligand and different analytes. Lowering the temperature reduces the kinetic on and off rates. Low-temperature sensorgrams, therefore, exhibit more curvature, which can be used to differentiate kinetic traces. This is especially significant for the IgG–FcγRII interaction because it is known to produce very fast "box-like" SPR sensorgrams at room temperature. To apply our previous findings to the IgG–FcγR interactions, we injected all TZM glycoforms at the same concentration (300 nM) at both 5°C and 25°C over FcγRIIA and FcγRIIB (Figure 2). For both receptors, the sensorgrams recorded at 25°C were almost perfectly overlaid, while some differences were qualitatively observed at 5°C, especially in the dissociation phase of the sensorgrams. TZM-GT exhibited a slower dissociation from FcγRIIA, while the three afucosylated glycoforms (Afuc1, Afuc2, Afuc3) dissociated from FcγRIIB with a slower rate. The kinetic differences were also more discernible at 5°C for both FcγRIII receptors tested (V158 and F158), with the afucosylated glycoforms dissociating the slowest (see Supporting Information S1: Figure S2). We performed all further experiments at 5°C, aiming to quantify these differences.

3.3 | The affinity of the IgG-FcγRIIA/B interaction depends on the IgG N-glycosylation

We injected each TZM glycoform at multiple concentrations between 10 and 1000 nM at 5°C over FcγRIIA and FcγRIIB surfaces (Figure 3). The thermodynamic constants ($K_D = 1/K_A$) were obtained by averaging the SPR signal during the last 2 s of the association phase, deemed to be representative of the equilibrium.

TZM-GT exhibited the highest affinity for FcγRIIA. In general, the afucosylated glycoforms showed a lower affinity for FcγRIIA than the fucosylated ones. The opposite is true for FcγRIIB. As such, even if the differences remain small, one might be able to make several inferences on the glycosylation profile by measuring the affinity for FcγRII receptors. However, this approach would require the injection of multiple antibody concentrations and sufficient association times to reach equilibrium, which is longer at low experimental temperatures. This also presupposes knowledge of the antibody concentration.

We performed the same experiments with FcγRIII receptors (see Supporting Information S1: Figure S3). Matching the findings of previous reports (Cambay et al., 2019, 2020; Falconer et al., 2018; Forest-Nault et al., 2021; Kanda et al., 2007; Okazaki et al., 2004; Shibata-Koyama et al., 2009; Subedi & Barb, 2016), these receptors exhibited an eightfold stronger affinity to IgGs which are afucosylated, compared to wild-type. However, it took approximately 10 times longer to reach equilibrium, thus requiring approximately 10 times more antibodies.

3.4 | The dissociation phase of a normalized SPR signal is independent of analyte concentration

We suggest computing the AUC during the dissociation phase of the normalized SPR sensorgrams to quantify differences in SPR signals. Two reasons guide our proposal. First, it is not specifically necessary to achieve equilibrium during the association phase to compute the AUC. While not a significant issue with FcγRII, achieving equilibrium demands long injection times for FcγRIII, especially at low temperatures. Second, for a given association time, the dissociation phase signal should be independent of the analyte concentration. Thus, injecting multiple antibody concentrations is not required. In fact, as shown in Figure 4, the dissociation curves obtained with the same

10970290, 0, Downloaded from https://analyticalsciencejournals.onlinelibrary.wiley.com/doi/10.1002/bit.28673 by Ecole Polytech De Montreal, Wiley Online Library on [18/03/2024]. See the Terms and Conditions (https://onlinelibrary.wiley.com/terms-and-conditions) on Wiley Online Library for rules of use; OA articles are governed by the applicable Creative Commons License

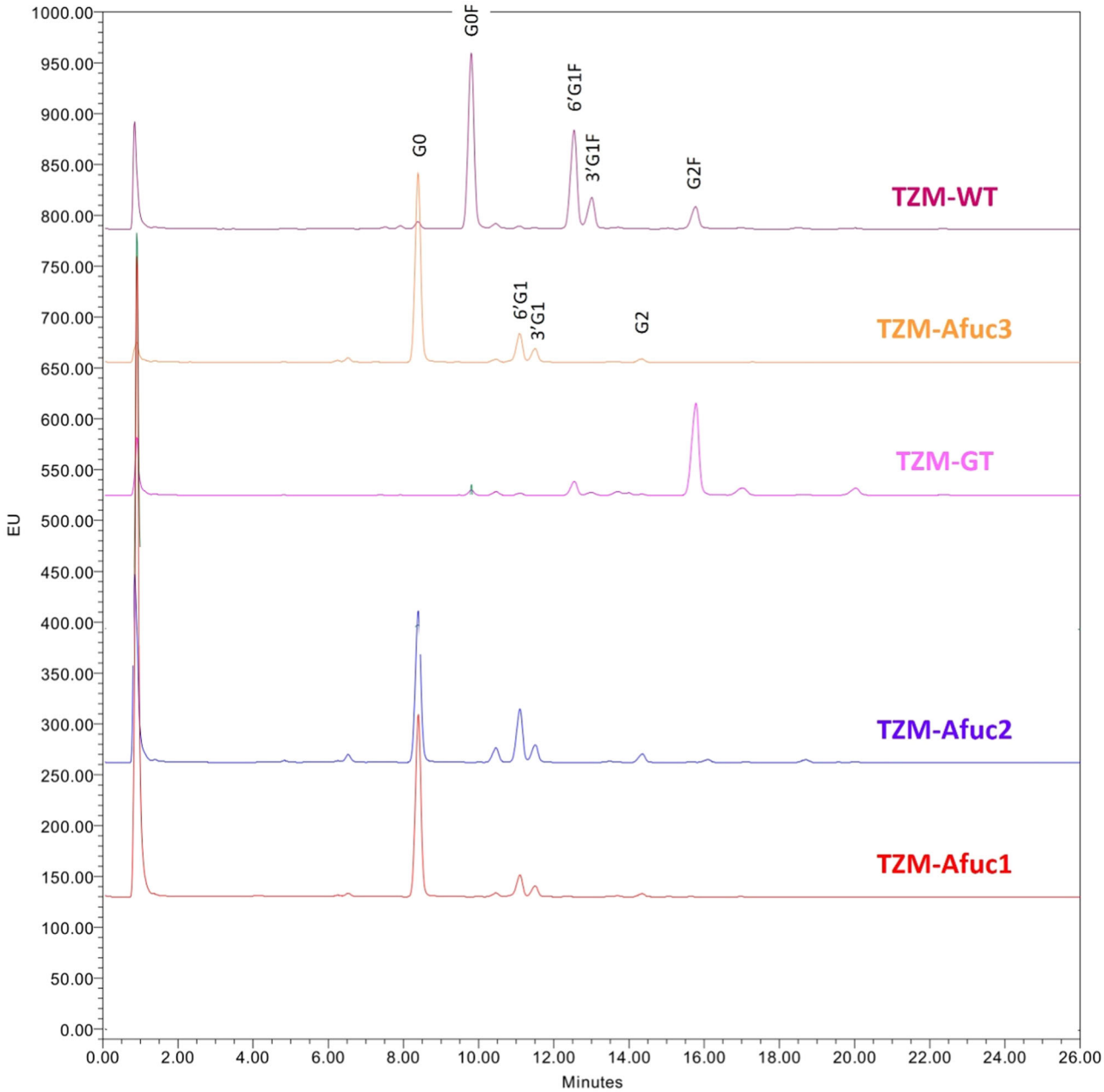

FIGURE 1 HILIC-UPLC analysis of the abundance of the N-linked glycans present in each of the *Trastuzumab* samples.

TABLE 1 Summary of the N-linked glycan analysis.

Sample	TZM-Afuc1	TZM-Afuc2	TZM-Afuc3	TZM-GT	TZM-WT
% Fucosylation	0	0	0	75.0	91.6
% Galactosylation	9.8	20	11.5	68.3	27.3
% High mannose	2.6	6	1.6	20.9	3.5
% Sialylation	0	1.4	0	0	0
% Unassigned	1.8	2.4	0.8	1.6	1.5

Abbreviations: GT, glycosyltransferase β1,4-galactosyltransferase 1; TZM, *Trastuzumab*; WT, wild-type.

antibody at various concentrations were nearly perfectly overlaid when normalized. This is not the case for the association phase, wherein the rate of IgG–FcγR complex formation is dependent on the antibody concentration.

3.5 | The AUC of the dissociation phase is a simple SPR signal discriminator

The AUC was computed numerically using the trapezoidal method. The glycoforms were injected in triplicates at 10, 30, 100, and 300 nM over FcγRIIA and FcγRIIB surfaces. As we previously

10970290, 0, Downloaded from https://analyticalsciencejournals.onlinelibrary.wiley.com/doi/10.1002/bit.28673 by Ecole Polytech De Montreal, Wiley Online Library on [18/03/2024]. See the Terms and Conditions (https://onlinelibrary.wiley.com/terms-and-conditions) on Wiley Online Library for rules of use; OA articles are governed by the applicable Creative Commons License

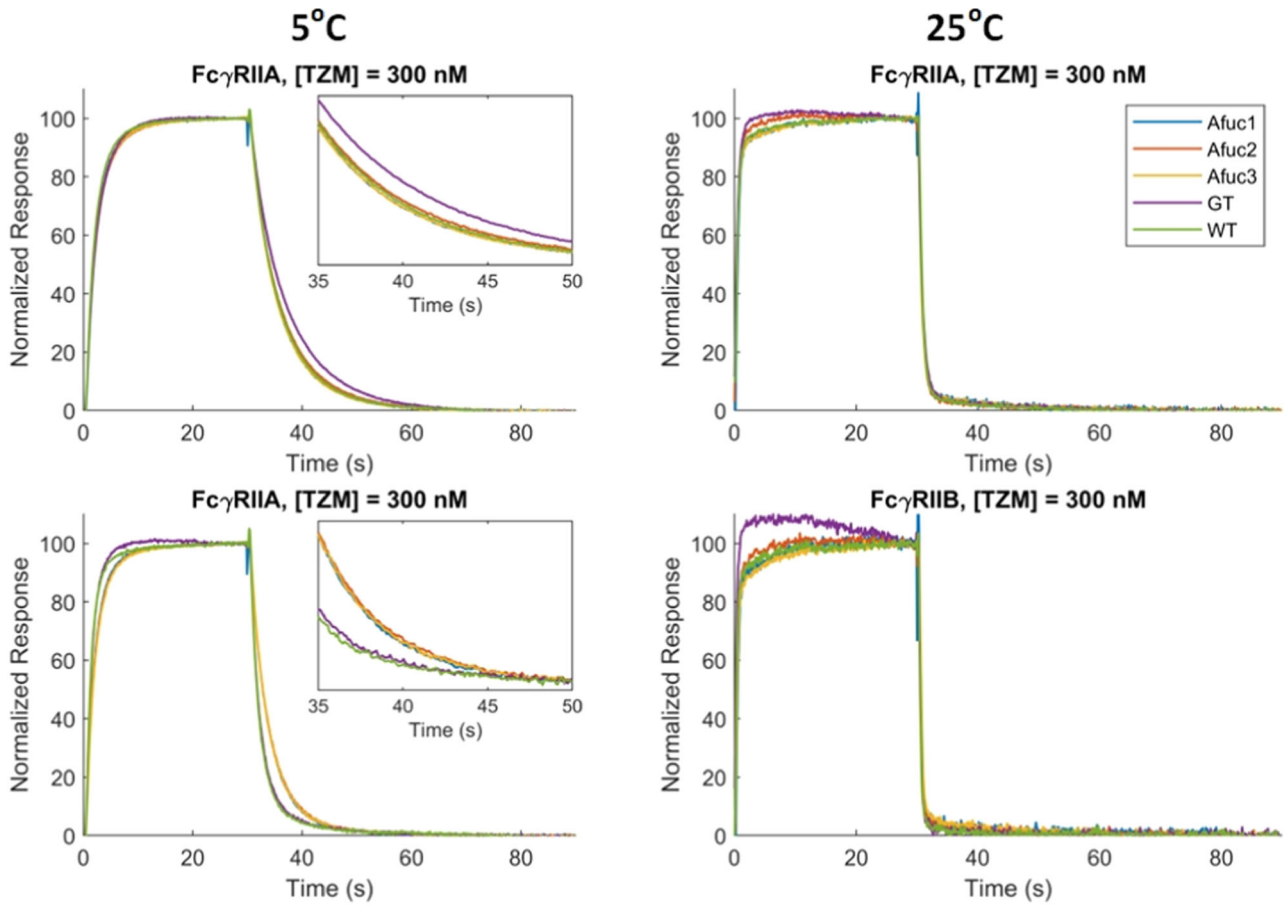

FIGURE 2 Overlay of the normalized surface plasmon resonance (SPR) sensorgrams obtained by capturing either Fcγ receptor (FcγR)IIA (top) or FcγRIIB (bottom) on the SPR surface and injecting five glycoforms of *Trastuzumab* at 300 nM, setting the experimental temperature at either 5°C (left) or 25°C (right). Insets on the 5°C graphs show a zoomed-in view of the dissociation phase of the sensorgrams.

demonstrated (Figure 4), the dissociation signal measured with different antibody concentrations were overlaid when normalized. Thus, the same AUCs should be obtained for every concentration, meaning differences in AUCs between different TZM glycoforms should be observable for theoretically any antibody concentration, and knowledge of said concentration should be unnecessary. As such, using a lower concentration is desirable as it requires less antibody. However, the normalization to 100 RU of low amplitude sensorgrams significantly amplifies experimental noise. This results in wider confidence intervals for the AUCs in the case of sensorgrams with a low signal-to-noise ratio, complicating the glycoform discrimination.

The AUC computation results are shown in Figure 5. FcγRIIA exhibited an AUC with TZM-GT that was significantly greater than with all other glycoforms at 30, 100, and 300 nM (Figure 5b,c,d). Other glycoforms showed no significant differences between themselves, clearly indicating that the galactosylation level was the differentiating factor. The AUCs of FcγRIIB obtained with TZM-WT and TZM-GT (fucosylated) were smaller than those obtained with the afucosylated glycoforms (TZM-Afuc1, TZM-Afuc2, and TZM-Afuc3). The differences were significant when the antibody concentration injected was 100 nM or higher (Figure 5g,h). The differences in the width of the error bars can be explained by differences in signal amplitude, as stronger signals tend to lead to a more precise AUC computation. From the amplitude reached by the unnormalized SPR signals at the end of the association phase, indicated in white on the bars of Figure 5, we deduce that significant differences were observed when the SPR signal recorded at the end of the association phase was greater than 10 RU. Considering a standard deviation of 0.2 RU for the measurement noise of the Biacore T100 biosensor (computed by taking the standard deviation of the baseline signal over 1 min), this corresponds to a signal-to-noise ratio of 50. Hence, FcγRIIA and FcγRIIB can be used respectively to detect galactosylation and fucosylation of IgGs.

3.6 | The AUC can be used as a quantitative metric for percent galactosylation and fucosylation inference

TZM-WT, TZM-GT, and TZM-Afuc3 were mixed pairwise at various ratios and were injected at 300 nM over captured FcγRIIA and FcγRIIB. The AUCs corresponding to these sensorgrams as well as those obtained by injecting these TZM lots alone are shown in

10970290, 0, Downloaded from https://analyticalsciencejournals.onlinelibrary.wiley.com/doi/10.1002/bit.28673 by Ecole Polytech De Montreal, Wiley Online Library on [18/03/2024]. See the Terms and Conditions (https://onlinelibrary.wiley.com/terms-and-conditions) on Wiley Online Library for rules of use; OA articles are governed by the applicable Creative Commons License

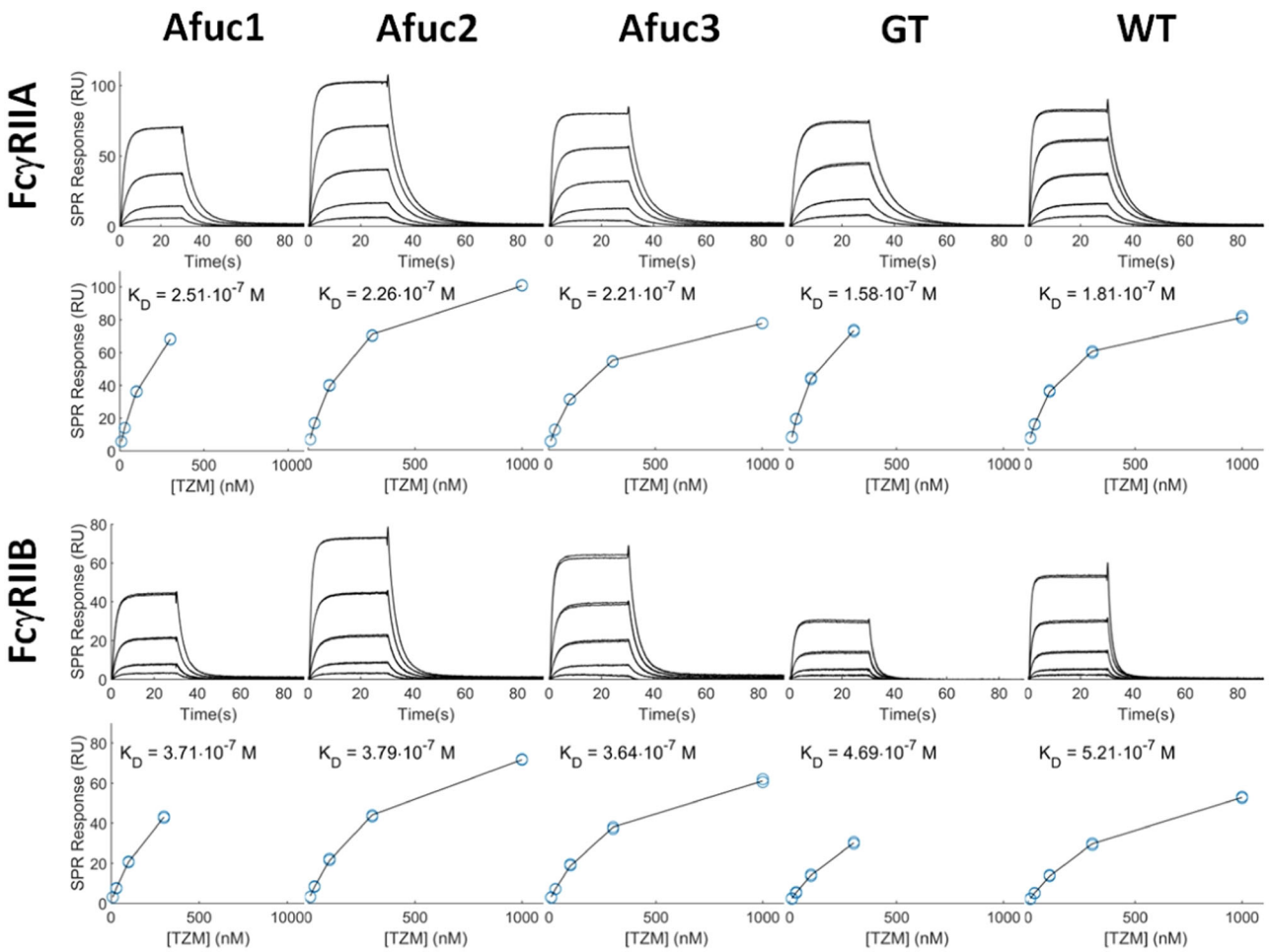

FIGURE 3 Surface plasmon resonance sensorgrams recorded at 5°C. Each set of sensorgrams was recorded by capturing ~20 RU of E-coil tagged Fcγ receptor (FcγR)IIA or FcγRIIB and injecting a concentration series of a *Trastuzumab* (TZM) glycoform in duplicate, according to the plot titles. The TZM glycoforms were injected at 10, 30, 100, and 300 nM (Afuc1 and GT) or 10, 30, 100, 300, and 1000 nM (Afuc2, Afuc3, wild-type). Under each set of sensorgrams is the corresponding steady-state model fit, with the identified thermodynamic constant K_D indicated on the plots.

Figure 6. This figure shows a linear relationship between the AUC measurements with FcγRIIA and the percentage of galactosylated TZM glycoforms (as measured by HILIC-UPLC) (Figure 6a) and between the percentage of fucosylation and the AUC measured with FcγRIIB (Figure 6b). Figure 6a shows a positive trend, meaning that galactose contributes to slowing the dissociation of IgGs from FcγRIIA, thus increasing the AUC. The linear trend of Figure 6a mainly comes from the GT-WT mixtures (in purple) and the Afuc-GT mixtures (in cyan), as these mixtures contain TZM-GT, which is the most galactosylated lot. Afuc-WT mixtures (in green) show little differences in galactosylation and AUC, and as such the corresponding data points deviate slightly from the linear trend. Figure 6b shows a negative trend, indicating that the presence of fucose accelerates the dissociation of IgGs from FcγRIIB, leading to a decrease in AUC. This is mainly observed with the Afuc-WT and Afuc-GT mixtures. The GT-WT mixtures show small differences in AUC, as TZM-GT and TZM-WT are both heavily fucosylated. Overall, Figure 6 shows that, with proper referencing and normalization, FcγRIIA/B can be used to quantitatively infer the abundance of galactosylated and fucosylated glycoforms with satisfactory precision.

4 | DISCUSSION

In this study, we showed that performing low-temperature SPR experiments using immobilized FcγRIIA allows for the discrimination of galactosylated IgG1 glycoforms, while immobilized FcγRIIB allows discrimination of fucosylated glycoforms. Quantification of the proportion of galactosylated or fucosylated glycoforms is possible by computing the AUC of the dissociation phase signal of the normalized sensorgrams.

We produced different glycoforms of TZM, an IgG1, using glycoengineering methods and finely characterized them (see Figure 1 and Table 1). The main differences were in their core fucosylation and galactosylation levels. The interaction kinetics of these glycoforms for various FcγRs were recorded using a robust and

10970290, 0, Downloaded from https://analyticalsciencejournals.onlinelibrary.wiley.com/doi/10.1002/bit.28673 by Ecole Polytech De Montreal, Wiley Online Library on [18/03/2024]. See the Terms and Conditions (https://onlinelibrary.wiley.com/terms-and-conditions) on Wiley Online Library for rules of use; OA articles are governed by the applicable Creative Commons License

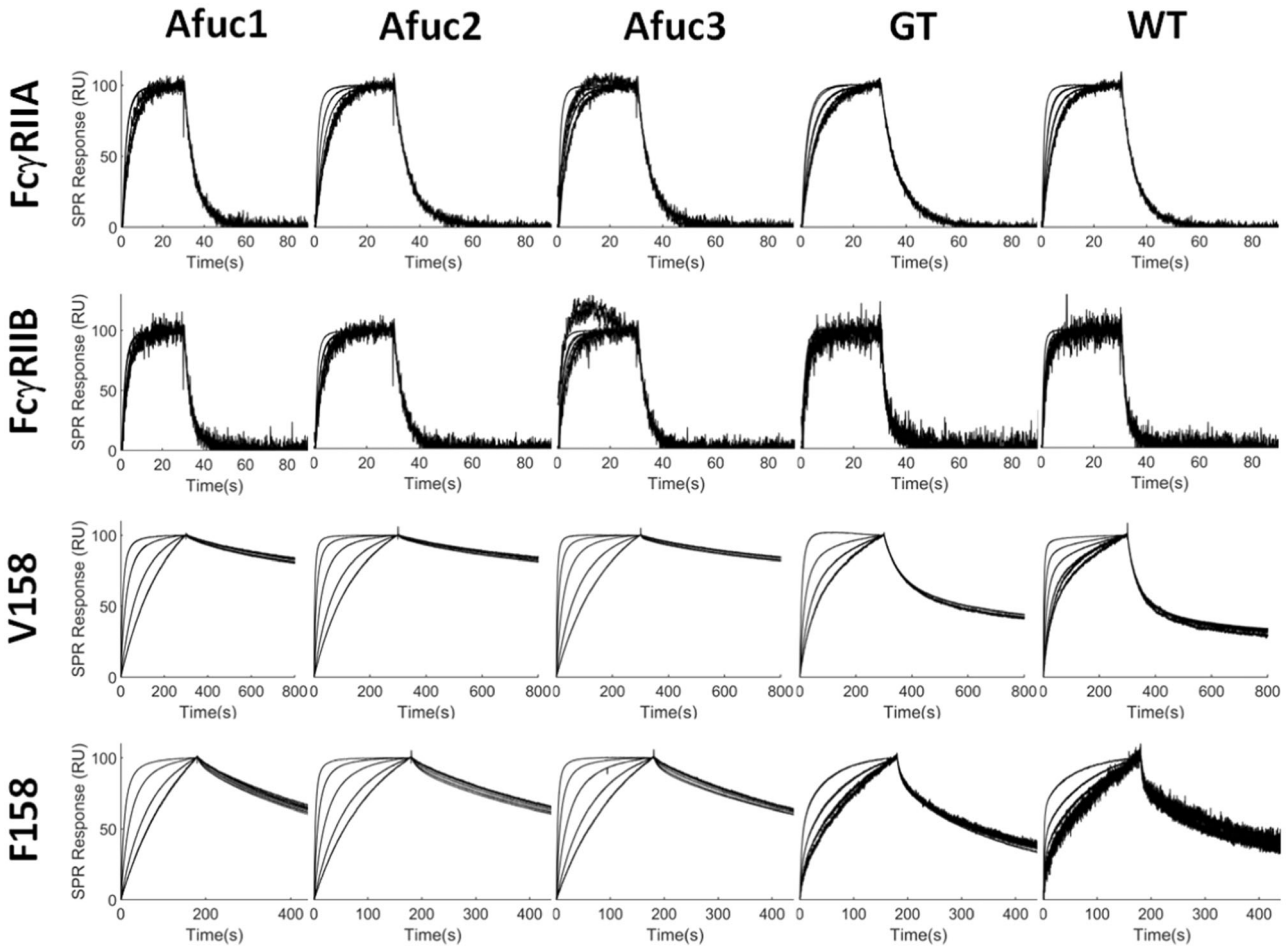

FIGURE 4 Overlay of normalized surface plasmon resonance sensorgrams obtained at different antibody concentrations for all *Trastuzumab* glycoforms (Afuc1, Afuc2, Afuc3, glycosyltransferase β1,4-galactosyltransferase 1 [GT], and wild-type [WT]) and all Fcγ receptors (FcγRs) used in this study (FcγRIIA, FcγRIIB, V158 for FcγRIIIA with a valine at position 158 and F158 for FcγRIIIA with a phenylalanine at position 158). The plot titles indicate the corresponding glycoform and receptor. Afuc1 and GT were injected at four concentrations (10, 30, 100, and 300 nM) whereas Afuc2, Afuc3, and WT were injected at five concentrations (10, 30, 100, 300, and 1000 nM). The signals were normalized such that a response of 100 RU is reached at the end of the association phase.

repeatable coiled-coil-based SPR assay so that trends observed in this study may not be attributed to ligand immobilization biases. Of interest, we found that decreasing the SPR experimental temperature amplified the differences in the binding behavior of FcγRs to differentially glycosylated TZM lots (Figure 2). Temperature dependence is especially crucial for FcγRIIA/B, as their associated kinetics are very fast and show little curvature at room temperature. At 5°C, we qualitatively observed a slower dissociation between FcγRIIA and TZM-GT, indicating that FcγRIIA could be used to detect differences in galactosylation levels. Similarly, we observed a slower dissociation from FcγRIIB for all afucosylated glycoforms, indicating that FcγRIIB could detect fucosylation. These findings were quantified by injecting a concentration series of each glycoform over both receptors to deduce the interaction affinity at 5°C (Figure 3).

However, affinity calculation requires multiple SPR cycles and knowledge of the antibody concentration. We thought a quicker and less data-demanding glycosylation discrimination method would be to compute the AUC of the dissociation phase of the SPR sensorgrams. Indeed, when normalized, the dissociation phase signal is independent of the antibody concentration (Figure 4). Hence, only one sensorgram, at theoretically any concentration, would be needed to detect galactosylation or fucosylation levels (Figure 5). One can also use the AUC with FcγRIIA/B to quantify the abundance of galactosylated and fucosylated glycoforms in a given sample, as linear relations were found between the AUC and the percent galactosylation/fucosylation in an IgG sample (Figure 6).

The vast majority of IgG–FcγR SPR experiments reported in the literature were performed at room temperature. Yet temperature control is a standard feature of most commercial SPR biosensors. Performing SPR experiments at a lower temperature slows down the association and dissociation kinetic rates. Interactions that are too fast to properly differentiate at room temperature may exhibit an appreciable degree of curvature at 5°C, and differences may be unraveled. This was the case for the IgG-FcγRIIA/B interaction, opening the way to discriminate antibody glycoforms with these receptors. Lowering the temperature slows down the kinetics, which

10970290, 0, Downloaded from https://analyticalsciencejournals.onlinelibrary.wiley.com/doi/10.1002/bit.28673 by Ecole Polytech De Montreal, Wiley Online Library on [18/03/2024]. See the Terms and Conditions (https://onlinelibrary.wiley.com/terms-and-conditions) on Wiley Online Library for rules of use; OA articles are governed by the applicable Creative Commons License

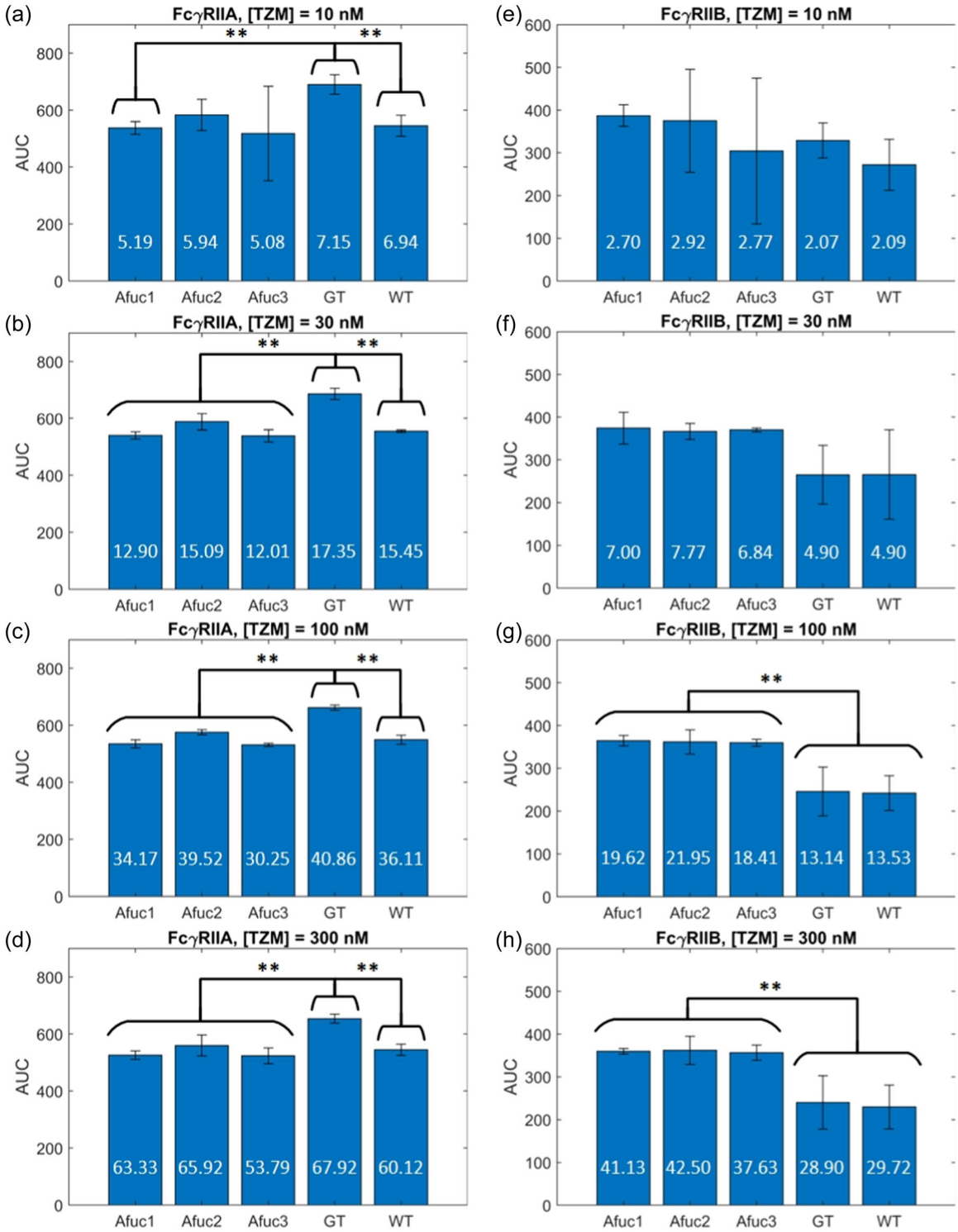

FIGURE 5 Area under the curve of the surface plasmon resonance signal during the dissociation phase of the sensorgrams. All five *Trastuzumab* (TZM) glycoforms (Afuc1, Afuc2, Afuc3, GT, and wild-type) were injected over captured Fcγ receptor (FcγR)IIA (a–d) and FcγRIIB (e–h) at four different concentrations (10, 30, 100, and 300 nM, rows) in triplicate. The 95% confidence intervals are depicted over each bar. Double stars (**) indicate significant differences (2-way student *t* test at a 95% confidence threshold). The signal amplitude (in RU) attained at the end of the association phase is indicated on each bar (average of the triplicates).

in theory would increase the time and sample volume required to reach equilibrium and for complete dissociation. However, this was not limiting with FcγRII receptors as their kinetics remain very fast (a 30 s association and a 60 s dissociation are sufficient, even at 5°C), meaning a result can be recorded in just a few minutes. SPR instruments require a very low sample volume to obtain one sensorgram. As such, our proposed method can discriminate between high and low levels of galactosylation and fucosylation using a very

10970290, 0, Downloaded from https://analyticalsciencejournals.onlinelibrary.wiley.com/doi/10.1002/bit.28673 by Ecole Polytech De Montreal, Wiley Online Library on [18/03/2024]. See the Terms and Conditions (https://onlinelibrary.wiley.com/terms-and-conditions) on Wiley Online Library for rules of use; OA articles are governed by the applicable Creative Commons License

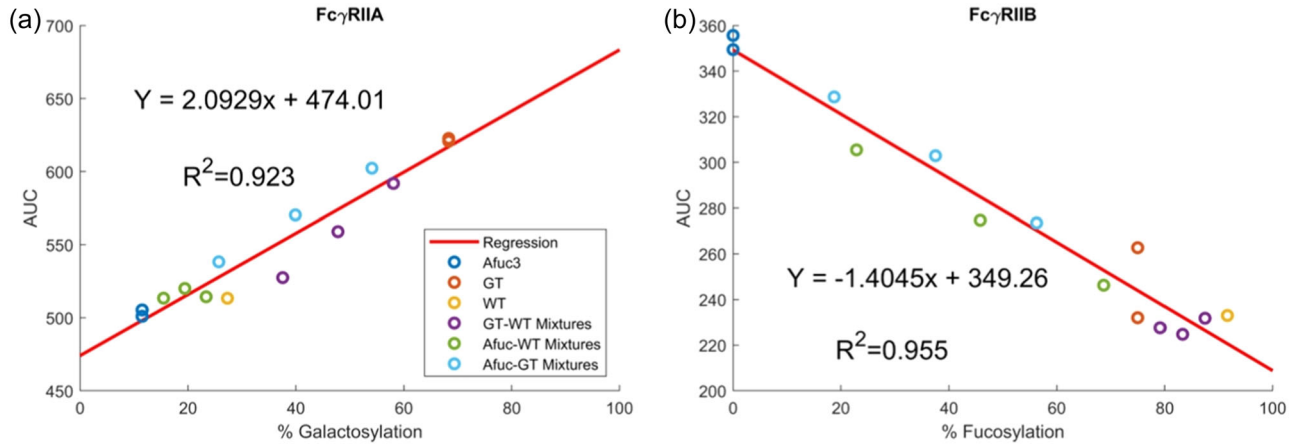

FIGURE 6 Linear regression of the area under the curve computed from sensorgrams obtained by injecting 300 nM solutions of *Trastuzumab* (TZM) glycoforms on captured Fcγ receptor (FcγR)IIA (a) and FcγRIIB (b) with respect to the percentage of galactosylated antibodies (a) and fucosylated antibodies (b). The linear regression equation of each graph is indicated on the graphs as well as the coefficient of determination (R^2). GT-wild-type (WT) and Afuc-WT mixtures are mixtures containing 25%, 50%, and 75% of TZM-GT or TZM-Afuc3 with the remainder being TZM-WT. Afuc-GT mixtures are mixtures containing 25%, 50%, and 75% of TZM-Afuc3 with the remainder being TZM-GT.

small quantity of antibodies (approximately 250 ng for one sensorgram at 100 nM).

We previously demonstrated that reducing the experimental temperature can facilitate the fit to a 1:1 model for SARS-CoV-2 SPR data (Forest-Nault et al., 2022), and that reducing the temperature increases differences between sensorgrams obtained by injecting various analytes of a model Carbonic Anhydrase II-based system (Gaudreault et al., 2022), but to our knowledge this is the first study that utilizes temperature as a means to amplify kinetic differences between MAb glycoforms.

The IgG–FcγR interaction does not fit well to a simple 1:1 Langmuir model (Forest-Nault et al., 2021). Hence, kinetic parameters obtained from such models are not reliable and should not constitute the basis of a glycosylation inference method. An observed affinity can be computed for most complex interaction schemes, but this requires injecting the antibody at multiple known concentrations. In stark contrast, our proposed method theoretically only requires one antibody injection, and knowledge of the concentration is not even necessary. In fact, concentrations as low as 30 nM may be sufficient for differentiation. The amplitude of the SPR signal at the end of the association phase determines the signal-to-noise ratio, as the instrument noise is independent of signal amplitude. A signal-to-noise ratio of 50 was deemed sufficient to obtain significant differences (corresponding to a response of 10 RU at the end of the association phase for the Biacore T100 used in this study). If the signal-to-noise ratio is too low to yield significant differences in AUC, a second injection at a higher antibody concentration may be necessary. Alternatively, the immobilized density of receptor could be increased, as long as the system does not become mass transport limited.

Most SPR dissociation phase models, from the simple 1:1 Langmuir model to the N heterogeneous analyte models, can be simplified to a sum of decaying exponentials. Herein, the coefficients depend on the observed binding affinities and their respective contributions to the signal at the end of the association phase, while the exponents correspond to the dissociation rates involved (Gaudreault et al., 2022; Gaudreault, Liberelle, et al., 2021). The integral of the dissociation phase signal is a function of those parameters, regardless of the actual interaction scheme. As such, the AUC is a metric that allows comparison of different samples by encompassing information on the composition of the sample and the affinities and dissociation rates in play.

On top of the novel findings reported at 5°C with FcγRIIA/B, results that are well-known and widely reported were also obtained with the AUC method. Indeed, a much larger AUC was obtained with FcγRIIIA (both V158 and F158) and afucosylated IgG1 glcyoforms than with fucosylated samples. This corroborates reports of an increased affinity by up to more than 10-fold when core fucose is absent (Cambay et al., 2019, 2020; Falconer et al., 2018; Forest-Nault et al., 2021; Kanda et al., 2007; Okazaki et al., 2004; Shibata-Koyama et al., 2009; Subedi & Barb, 2016). This observation validates the AUC as a method for glycosylation discrimination. It is, however, noteworthy that FcγRIIA/B reaches equilibrium much faster than FcγRIIIA, making the former a more interesting option for experiments at low temperatures. Moreover, although the AUC is simple because it is quantitative, it allows inferences on the glycan abundance.

Glycosylation assessment methods based on chromatography can precisely differentiate between different glycan chains, whereas our method can only discriminate the presence or absence of galactose and core fucose, independently from the rest of the glycans present in the chains. Impressive repeatability and robustness have been reported with high throughput chromatography-based methods in the literature, with coefficients of variation of a few percentage points over hundreds of experiments (Deriš et al., 2021). Therefore, the advantage of the AUC as measured with SPR resides in its

10970290, 0, Downloaded from https://analyticalsciencejournals.onlinelibrary.wiley.com/doi/10.1002/bit.28673 by Ecole Polytech De Montreal, Wiley Online Library on [18/03/2024]. See the Terms and Conditions (https://onlinelibrary.wiley.com/terms-and-conditions) on Wiley Online Library for rules of use; OA articles are governed by the applicable Creative Commons License

rapidity (approximately 5 min per SPR measurement, as opposed to the 2 h reported by Deriš et al.) and the reduced sample preprocessing (SPR does not require labeling, nor deglycosylation).

5 | CONCLUSION

A tool for antibody N-glycosylation monitoring is of great interest in both research and industrial settings, as glycosylation is a critical quality attribute of MAbs. Considering the inherent advantages of SPR, such as low sample volume requirement, label-free detection, real-time measurement, and fast data acquisition, it is a promising monitoring tool that can be applied all the way from upstream production to downstream purification. The suggested analytical framework can provide at least a qualitative detection of the prevalence of fucosylated and galactosylated IgG glycoforms in a sample, and at best a quantitative percentage of antibody-heavy chains harboring these glycans. Such a quantification can be obtained with two SPR sensorgrams (one for each FcγRII) requiring only a few minutes. This is much faster and requires less manipulations compared to other qualitative methods, such as lectin blotting, or quantitative methods, such as mass spectrometry and high-performance liquid chromatography. The AUC method is faster than traditional SPR-based approaches, as fewer sensorgrams are needed.

Most SPR instruments have multiple distinct surfaces where one can immobilize ligands. This opens the way to assays capable of evaluating multiple attributes with a single analyte injection. For example, two surfaces could harbor FcγRIIA and FcγRIIB to detect galactosylation and fucosylation, respectively, and another could harbor the antigen to evaluate the antibody bioactivity and/or its titer, depending on the antigen immobilization density. Another surface would be kept as a blank for referencing purposes. Such integrated assays will be key for SPR-based bioprocess monitoring.

AUTHOR CONTRIBUTIONS

Jimmy Gaudreault performed all SPR experiments and data analysis. Catherine Forest-Nault performed cell culture and protein purification. Michel Gilbert was responsible for HILIC-UPLC glycan analysis. Yves Durocher provided mentorship. Olivier Henry and Gregory De Crescenzo contributed equally to the supervision of this work. All authors reviewed the manuscript.

ACKNOWLEDGMENTS

This work was supported by the Natural Sciences and Engineering Research Council of Canada (stipends allocated to J. G. and C. F. -N. including one from the PrEEmiuM CREATE program). The authors would like to thank Benjamin Serafin for fruitful discussions and revisions during the writing of the manuscript.

DATA AVAILABILITY STATEMENT

The data that support the findings of this study are available from the corresponding author upon reasonable request.

ORCID

Olivier Henry http://orcid.org/0000-0003-2106-1331
Gregory De Crescenzo http://orcid.org/0000-0002-6280-1570

REFERENCES

Bigge, J. C., Patel, T. P., Bruce, J. A., Goulding, P. N., Charles, S. M., & Parekh, R. B. (1995). Nonselective and efficient fluorescent labeling of glycans using 2-amino benzamide and anthranilic acid. *Analytical Biochemistry*, *230*(2), 229–238. https://doi.org/10.1006/abio.1995.1468

Boune, S., Hu, P., Epstein, A. L., & Khawli, L. A. (2020). Principles of N-linked glycosylation variations of IgG-based therapeutics: Pharmacokinetic and functional considerations. *Antibodies (Basel, Switzerland)*, *9*(2), 22. https://doi.org/10.3390/antib9020022

Cambay, F., Forest-Nault, C., Dumoulin, L., Seguin, A., Henry, O., Durocher, Y., & De Crescenzo, G. (2020). Glycosylation of Fcγ receptors influences their interaction with various IgG1 glycoforms. *Molecular Immunology*, *121*, 144–158. https://doi.org/10.1016/j.molimm.2020.03.010

Cambay, F., Henry, O., Durocher, Y., & De Crescenzo, G. (2019). Impact of N-glycosylation on Fcγ receptor/IgG interactions: Unravelling differences with an enhanced surface plasmon resonance biosensor assay based on coiled-coil interactions. *mAbs*, *11*(3), 435–452. https://doi.org/10.1080/19420862.2019.1581017

Carrara, S. C., Ulitzka, M., Grzeschik, J., Kornmann, H., Hock, B., & Kolmar, H. (2021). From cell line development to the formulated drug product: The art of manufacturing therapeutic monoclonal antibodies. *International Journal of Pharmaceutics*, *594*, 120164. https://doi.org/10.1016/j.ijpharm.2020.120164

Chavane, N., Jacquemart, R., Hoemann, C. D., Jolicoeur, M., & De Crescenzo, G. (2008). At-line quantification of bioactive antibody in bioreactor by surface plasmon resonance using epitope detection. *Analytical Biochemistry*, *378*(2), 158–165. https://doi.org/10.1016/j.ab.2008.04.019

De Crescenzo, G., Boucher, C., Durocher, Y., & Jolicoeur, M. (2008). Kinetic characterization by surface plasmon resonance-based biosensors: Principle and emerging trends. *Cellular and Molecular Bioengineering*, *1*(4), 204–215. https://doi.org/10.1007/s12195-008-0035-5

Dégardin, M., Gaudreault, J., Oliverio, R., Serafin, B., Forest-Nault, C., Liberelle, B., & De Crescenzo, G. (2023). Grafting strategies of oxidation-prone coiled-coil peptides for protein capture in bioassays: Impact of orientation and the oxidation state. *ACS Omega*, *8*(31), 28301–28313. https://doi.org/10.1021/acsomega.3c02172

Deriš, H., Cindrić, A., Lauber, M., Petrović, T., Bielik, A., Taron, C. H., van Wingerden, M., Lauc, G., & Trbojević-Akmačić, I. (2021). Robustness and repeatability of GlycoWorks RapiFluor-MS IgG N-glycan profiling in a long-term high-throughput glycomic study. *Glycobiology*, *31*(9), 1062–1067. https://doi.org/10.1093/glycob/cwab050

Falconer, D. J., Subedi, G. P., Marcella, A. M., & Barb, A. W. (2018). Antibody fucosylation lowers the FcγRIIIa/CD16a affinity by limiting the conformations sampled by the N162-glycan. *ACS Chemical Biology*, *13*(8), 2179–2189. https://doi.org/10.1021/acschembio.8b00342

Farahavar, G., Abolmaali, S. S., Gholijani, N., & Nejatollahi, F. (2019). Antibody-guided nanomedicines as novel breakthrough therapeutic, diagnostic and theranostic tools. *Biomaterials Science*, *7*(10), 4000–4016. https://doi.org/10.1039/C9BM00931K

Forest-Nault, C., Gaudreault, J., Henry, O., Durocher, Y., & De Crescenzo, G. (2021). On the use of surface plasmon resonance biosensing to understand IgG-FcγR interactions. *International Journal of Molecular Sciences*, *22*(12):6616. https://doi.org/10.3390/ijms22126616

10970290, 0, Downloaded from https://analyticalsciencejournals.onlinelibrary.wiley.com/doi/10.1002/bit.28673 by Ecole Polytech De Montreal, Wiley Online Library on [18/03/2024]. See the Terms and Conditions (https://onlinelibrary.wiley.com/terms-and-conditions) on Wiley Online Library for rules of use; OA articles are governed by the applicable Creative Commons License

Forest-Nault, C., Koyuturk, I., Gaudreault, J., Pelletier, A., L'Abbé, D., Cass, B., Bisson, L., Burlacu, A., Delafosse, L., Stuible, M., Henry, O., De Crescenzo, G., & Durocher, Y. (2022). Impact of the temperature on the interactions between common variants of the SARS-CoV-2 receptor binding domain and the human ACE2. *Scientific Reports*, *12*(1), 11520. https://doi.org/10.1038/s41598-022-15215-5

Gaudreault, J., Durocher, Y., Henry, O., & De Crescenzo, G. (2022). Multi-temperature experiments to ease analysis of heterogeneous binder solutions by surface plasmon resonance biosensing. *Scientific Reports*, *12*(1), 14401. https://doi.org/10.1038/s41598-022-18450-y

Gaudreault, J., Forest-Nault, C., De Crescenzo, G., Durocher, Y., & Henry, O. (2021). On the use of surface plasmon resonance-based biosensors for advanced bioprocess monitoring. *Processes*, *9*(11):1996. https://doi.org/10.3390/pr9111996

Gaudreault, J., Liberelle, B., Durocher, Y., Henry, O., & De Crescenzo, G. (2021). Determination of the composition of heterogeneous binder solutions by surface plasmon resonance biosensing. *Scientific Reports*, *11*(1), 3685. https://doi.org/10.1038/s41598-021-83268-z

Ghaderi, D., Taylor, R. E., Padler-Karavani, V., Diaz, S., & Varki, A. (2010). Implications of the presence of N-glycolylneuraminic acid in recombinant therapeutic glycoproteins. *Nature Biotechnology*, *28*(8), 863–867. https://doi.org/10.1038/nbt.1651

Gherghescu, I., & Delgado-Charro, M. B. (2021). The biosimilar landscape: An overview of regulatory approvals by the EMA and FDA. *Pharmaceutics*, *13*(1):48. https://doi.org/10.3390/pharmaceutics13010048

Goetze, A. M., Liu, Y. D., Zhang, Z., Shah, B., Lee, E., Bondarenko, P. V., & Flynn, G. C. (2011). High-mannose glycans on the Fc region of therapeutic IgG antibodies increase serum clearance in humans. *Glycobiology*, *21*(7), 949–959. https://doi.org/10.1093/glycob/cwr027

Gyorgypal, A., & Chundawat, S. P. S. (2022). Integrated process analytical platform for automated monitoring of monoclonal antibody N-linked glycosylation. *Analytical Chemistry*, *94*(19), 6986–6995. https://doi.org/10.1021/acs.analchem.1c05396

Hodoniczky, J., Zheng, Y. Z., & James, D. C. (2005). Control of recombinant monoclonal antibody effector functions by Fc N-glycan remodeling in vitro. *Biotechnology Progress*, *21*(6), 1644–1652. https://doi.org/10.1021/bp050228w

Homola, J. (2003). Present and future of surface plasmon resonance biosensors. *Analytical and Bioanalytical Chemistry*, *377*(3), 528–539. https://doi.org/10.1007/s00216-003-2101-0

Hossler, P., Khattak, S. F., & Li, Z. J. (2009). Optimal and consistent protein glycosylation in mammalian cell culture. *Glycobiology*, *19*(9), 936–949. https://doi.org/10.1093/glycob/cwp079

Jacquemart, R., Chavane, N., Durocher, Y., Hoemann, C., De Crescenzo, G., & Jolicoeur, M. (2008). At-line monitoring of bioreactor protein production by surface plasmon resonance. *Biotechnology and Bioengineering*, *100*(1), 184–188. https://doi.org/10.1002/bit.21725

Kanda, Y., Yamada, T., Mori, K., Okazaki, A., Inoue, M., Kitajima-Miyama, K., Kuni-Kamochi, R., Nakano, R., Yano, K., Kakita, S., Shitara, K., & Satoh, M. (2007). Comparison of biological activity among nonfucosylated therapeutic IgG1 antibodies with three different N-linked Fc oligosaccharides: The high-mannose, hybrid, and complex types. *Glycobiology*, *17*(1), 104–118. https://doi.org/10.1093/glycob/cwl057

Kaur, H. (2021). Characterization of glycosylation in monoclonal antibodies and its importance in therapeutic antibody development. *Critical Reviews in Biotechnology*, *41*(2), 300–315. https://doi.org/10.1080/07388551.2020.1869684

Koyuturk, I., Kedia, S., Robotham, A., Star, A., Brochu, D., Sauvageau, J., Kelly, J., Gilbert, M., & Durocher, Y. (2022). High-level production of wild-type and oxidation-resistant recombinant alpha-1-antitrypsin in glycoengineered CHO cells. *Biotechnology and Bioengineering*, *119*(9), 2331–2344. https://doi.org/10.1002/bit.28129

Lakayan, D., Haselberg, R., Gahoual, R., Somsen, G. W., & Kool, J. (2018). Affinity profiling of monoclonal antibody and antibody-drug-conjugate preparations by coupled liquid chromatography-surface plasmon resonance biosensing. *Analytical and Bioanalytical Chemistry*, *410*(30), 7837–7848. https://doi.org/10.1007/s00216-018-1414-y

Lakayan, D., Haselberg, R., Niessen, W. M. A., Somsen, G. W., & Kool, J. (2016). On-line coupling of surface plasmon resonance optical sensing to size-exclusion chromatography for affinity assessment of antibody samples. *Journal of Chromatography A*, *1452*, 81–88. https://doi.org/10.1016/j.chroma.2016.05.033

Leeman, M., Albers, W. M., Bombera, R., Kuncova-Kallio, J., Tuppurainen, J., & Nilsson, L. (2021). Asymmetric flow field-flow fractionation coupled to surface plasmon resonance detection for analysis of therapeutic proteins in blood serum. *Analytical and Bioanalytical Chemistry*, *413*(1), 117–127. https://doi.org/10.1007/s00216-020-03011-x

Lyu, X., Zhao, Q., Hui, J., Wang, T., Lin, M., Wang, K., Zhang, J., Shentu, J., Dalby, P. A., Zhang, H., & Liu, B. (2022). The global landscape of approved antibody therapies. *Antibody Therapeutics*, *5*(4), 233–257. https://doi.org/10.1093/abt/tbac021

Moorkens, E., Vulto, A. G., & Huys, I. (2020). An overview of patents on therapeutic monoclonal antibodies in Europe: Are they a hurdle to biosimilar market entry. *mAbs*, *12*(1):1743517. https://doi.org/10.1080/19420862.2020.1743517

Mullard, A. (2021). FDA approves 100th monoclonal antibody product. *Nature Reviews Drug Discovery*, *20*(7), 491–495. https://doi.org/10.1038/d41573-021-00079-7

Murschel, F., Liberelle, B., St-Laurent, G., Jolicoeur, M., Durocher, Y., & De Crescenzo, G. (2013). Coiled-coil-mediated grafting of bioactive vascular endothelial growth factor. *Acta Biomaterialia*, *9*(6), 6806–6813. https://doi.org/10.1016/j.actbio.2013.02.032

Myszka, D. G. (1999). Improving biosensor analysis. *Journal of Molecular Recognition*, *12*(5), 279–284. https://doi.org/10.1002/(sici)1099-1352(199909/10)12:5<279::Aid-jmr473>3.0.Co;2-3

Okazaki, A., Shoji-Hosaka, E., Nakamura, K., Wakitani, M., Uchida, K., Kakita, S., Tsumoto, K., Kumagai, I., & Shitara, K. (2004). Fucose depletion from human IgG1 oligosaccharide enhances binding enthalpy and association rate between IgG1 and FcγRIIIa. *Journal of Molecular Biology*, *336*(5), 1239–1249. https://doi.org/10.1016/j.jmb.2004.01.007

Shade, K. T., & Anthony, R. (2013). Antibody glycosylation and inflammation. *Antibodies*, *2*(3), 392–414.

Shibata-Koyama, M., Iida, S., Okazaki, A., Mori, K., Kitajima-Miyama, K., Saitou, S., Kakita, S., Kanda, Y., Shitara, K., Kato, K., & Satoh, M. (2008). The N-linked oligosaccharide at Fc RIIIa Asn-45: An inhibitory element for high Fc RIIIa binding affinity to IgG glycoforms lacking core fucosylation. *Glycobiology*, *19*(2), 126–134. https://doi.org/10.1093/glycob/cwn110

Stuible, M., Gervais, C., Lord-Dufour, S., Perret, S., L'Abbé, D., Schrag, J., St-Laurent, G., & Durocher, Y. (2021). Rapid, high-yield production of full-length SARS-CoV-2 spike ectodomain by transient gene expression in CHO cells. *Journal of Biotechnology*, *326*, 21–27. https://doi.org/10.1016/j.jbiotec.2020.12.005

Subedi, G. P., & Barb, A. W. (2016). The immunoglobulin G1 N-glycan composition affects binding to each low affinity Fc γ receptor. *mAbs*, *8*(8), 1512–1524. https://doi.org/10.1080/19420862.2016.1218586

Tharmalingam, T., Wu, C. H., Callahan, S., & T. Goudar, C. (2015). A framework for real-time glycosylation monitoring (RT-GM) in mammalian cell culture. *Biotechnology and Bioengineering*, *112*(6), 1146–1154. https://doi.org/10.1002/bit.25520

Umabs. (2023). *UmabsDB - the antibody therapies database*. https://umabs.com/

U. S. Food and Drug Administration. (2004). *Guidance for industry: PAT—A framework for innovative pharmaceutical development, manufacturing, and quality assurance*. U. S. Food and Drugs Administration.

U. S. Food and Drug Administration. (2009). *Guidance for industry: Q8(R2) pharmaceutical development*. U. S. Food and Drugs Administration.

10970290, 0, Downloaded from https://analyticalsciencejournals.onlinelibrary.wiley.com/doi/10.1002/bit.28673 by Ecole Polytech De Montreal, Wiley Online Library on [18/03/2024]. See the Terms and Conditions (https://onlinelibrary.wiley.com/terms-and-conditions) on Wiley Online Library for rules of use; OA articles are governed by the applicable Creative Commons License

Varki, A. (2017). Biological roles of glycans. *Glycobiology*, *27*(1), 3–49. https://doi.org/10.1093/glycob/cww086

Yamane-Ohnuki, N., Kinoshita, S., Inoue-Urakubo, M., Kusunoki, M., Iida, S., Nakano, R., Wakitani, M., Niwa, R., Sakurada, M., Uchida, K., Shitara, K., & Satoh, M. (2004). Establishment of FUT8knockout Chinese hamster ovary cells: An ideal host cell line for producing completely defucosylated antibodies with enhanced antibody-dependent cellular cytotoxicity. *Biotechnology and Bioengineering*, *87*(5), 614–622. https://doi.org/10.1002/bit.20151

Zhang, J., Liu, X., Bell, A., To, R., Baral, T. N., Azizi, A., Li, J., Cass, B., & Durocher, Y. (2009). Transient expression and purification of chimeric heavy chain antibodies. *Protein Expression and Purification*, *65*(1), 77–82. https://doi.org/10.1016/j.pep.2008.10.011

SUPPORTING INFORMATION

Additional supporting information can be found online in the Supporting Information section at the end of this article.

How to cite this article: Gaudreault, J., Forest-Nault, C., Gilbert, M., Durocher, Y., Henry, O., & De Crescenzo, G. (2024). A low-temperature SPR-based assay for monoclonal antibody galactosylation and fucosylation assessment using FcγRIIA/B. *Biotechnology and Bioengineering*, 1–15. https://doi.org/10.1002/bit.28673

10970290, 0, Downloaded from https://analyticalsciencejournals.onlinelibrary.wiley.com/doi/10.1002/bit.28673 by Ecole Polytech De Montreal, Wiley Online Library on [18/03/2024]. See the Terms and Conditions (https://onlinelibrary.wiley.com/terms-and-conditions) on Wiley Online Library for rules of use; OA articles are governed by the applicable Creative Commons License